Computational Assessment of the Entropy of Solvation of Small-Sized Hydrophobic Entities

Reema Mahajan,[a] Dieter Kranzlmüller,[b] Jens Volkert,[b]
Ulrich H. E. Hansmann[c,d] and Siegfried Höfinger[c]

[a] Indian Institute of Technology, Delhi,
Department of Chemical Engineering,
Hauz Khas, New Delhi-16, India.
E-mail: reema.mahajan@gmail.com

[b] Johannes Kepler University of Linz
, Institute of Graphics and Parallel Processing,
Altenberger Straße 69, A-4040, Linz, Austria.
E-mail: {kranzlmueller, volkert}@gup.jku.at

[c] Michigan Technological University,
Department of Physics,
1400 Townsend Drive, Houghton, MI, 49331-1295,USA.
E-mail: {hansmann, shoefing}@mtu.edu

[d] John von Neumann Institute for Computing, FZ Jülich,
52425 Jülich, Germany.

February 2, 2008

A high level polarizable force field is used to study the temperature dependence of hydrophobic hydration of small-sized molecules from computer simulations. Molecular dynamics simulations of liquid water at various temperatures form the basis of free energy perturbation calculations that consider the onset and growth of a repulsive sphere. This repulsive sphere acts as a model construct for the hydrophobic species. In the present study an extension is pursued to all in all seven independent target temperatures starting close to the freezing point and ranging up to almost the boiling point of liquid water at standard conditions. Care is taken to maintain

proper physico-chemical model description by cross-checking to experimental water densities at the selected target temperatures. The polarizable force field description of molecular water turns out to be suitable throughout the entire temperature domain considered. Derivatives of the computed free energies of hydrophobic hydration with respect to the temperature give access to the changes in entropy. In practice the entropy differential is determined from the negative of the slope of tangential lines formed at a certain target temperature in the free energy profile. The obtained changes in entropy are of negative sign for small sized cavities, hence reconfirm basic ideas of the *Lum Chandler Weeks* theory on hydrophobic hydration of small-sized solutes.

1 Introduction

The hydrophobic effect is widely believed to play a decisive role in protein folding, one of the key challenges in biophysical science and research of today [1, 2, 3]. Theoretical studies on the hydrophobic effect are of great relevance to a broad range of biosciences and a deeper understanding of hydrophobicity could certainly have its beneficial influence on many central questions in current biophysical research. Among others, *Lum Chandler Weeks* (LCW) theory of hydrophobicity [4] has received widespread appreciation. LCW theory describes the hydrophobic effect in terms of reorganizational work due to maintainance of a hydrogen bond network established between individual water molecules. A difference is made between small-sized hydrophobic solutes (volume dependence) and large-sized hydrophobic solutes (surface area dependence). Water molecules are believed to re-arrange appropriately around small-sized hydrophobic solutes thereby inducing the formation of clathrate-like substructures without destruction of the hydrogen bond network. In contrast, large-sized hydrophobic solutes are thought to enforce a complete re-arrangement of the hydrogen bond network adjacent to the hydrophobic solute, which in turn leads to agglomeration, aggregation and precipitation of the large-sized hydrophobic molecules. Such a picture of hydrophobicity would render the change in entropy for the process of solvating small-sized hydrophobic solutes to be negative in sign (increase in order), and the opposite for large-sized hydrophobic molecules (decrease in order). Hence, two immediate questions arise naturally: i) can computer simulations verify the claim of entropic drop for hydration of small-sized hydrophobic solutes ? ii) are current model descriptions of molecular water able to reproduce the physics of hydrophobicity correctly ? Although complementary, these two questions have to be addressed by atomistic computer simulations of hydrophobic solutes in aqueous solution.

Computer simulations have become a valuable tool in the study of hydrophobicity [5, 6, 7, 8, 9]. Among other techniques, free energy calculations have been introduced and advanced to directly study ΔG trends for various physico-chemical processes [10, 11, 12]. One such possible process is to investigate the ΔG corresponding to the introduction, onset and growth of a repulsive

sphere located in the center of a simulation cell filled with water molecules. In such a model, the repulsive sphere stands as a representative of an artificial hydrophobic solute. The associated free energy change is known as the cavitation free energy, ΔG^{cav} [13]. Postma and coworkers have introduced this type of calculation as one of the early examples of *Free Energy Perturbation* calculations (FEP). Their approach is known as the *Overlapping Spheres Technique* (OST) [11]. Recent re-evaluations and variations of the OST in the context of hydrophobicity have been summarized in [14]. The advantage of true estimates of ΔG becomes evident when looking at the derivative with respect to temperature, $\frac{\partial}{\partial T}(\Delta G) = \frac{\partial}{\partial T}(\Delta H - T\Delta S) = -\Delta S$, i.e. from a record of different ΔG values at different temperatures the change in entropy can be determined from the negative slope of the tangent formed at a particular point. Thus if the LCW arguments hold true, then for solvating small-sized hydrophobic solutes one would obtain a bell-shaped curve of the temperature plot of ΔG, for otherwise the slope of the tangent at room temperature can not become positive, hence ΔS not negative. However, high temperature simulations in the molecular mechanics description need to be carefully cross-checked against experimental data whether they still can provide reasonable representations of the native state. Therefore, only if one can confirm that a set of high temperature simulations still takes place at reasonable physico-chemical conditions, an estimate of entropies can be obtained. For the type of atomistic interaction governing hydrophobic phenomena, a proper account of the liquid water density at high temperatures is the most essential precondition for pursuing estimates of the entropy [15, 16].

Model descriptions of water have a great influence on the outcome of biomolecular simulations [17, 18] but the employment of prominent water models [19, 20] is common practice in present biophysical research. A specific high level description of molecular water has been proposed with the use of polarizable models [21]. The just cited AMOEBA model has been shown to exhibit excellent description of the temperature and pressure dependence of water [22]. AMOEBA water was successfully applied in describing aspects of the hydrophobic effect [23]. Since this previous study was focussing on room temperature behavior, an extension towards high temperature repeats is straightforward as it could lead to new insight into fundamental principles of hydrophobicity. Other studies on the entropy of hydrophobic hydration were mainly based on rigid water models so far [24, 25].

The present article reports cavitation free energy calculations performed at seven individual temperatures in the range of 277 K to 370 K. The polarizable AMOEBA water model [21] is used and Ewald summation is applied within the *Molecular Dynamics* simulations (MD) that form the basis of the FEP calculation of the OST approach. Emphasis is placed on verification of proper physico-chemical model description at high temperatures by comparison to experimentally obtained trends of liquid water densities. Entropic changes for this process are derived from the temperature dependence, that is the entropy of hydrophobic hydration is estimated by means of computer simulations. The computational demand of this study is on the order of three CPU years on decent architectures (Itanium 1.4 GHz) [26] and can only be

satisfied from massive employment of grid computing systems, such as for example the Austrian grid [27].

2 Methods

2.1 Simulation Cell Set Up

Seven individual cubic boxes composed of 6 x 6 x 6 grid cells were formed, where the sub-volume of the grid cells was adjusted to reproduce the experimental liquid water density corresponding to a chosen target temperature. Seven target temperatures were selected, 277 K, 300 K, 315 K, 330 K, 345 K, 365 K and 370 K. The structure of a single water molecule was optimized and then periodically translated and copied to each of the centers of the grid cells. Thus all simulation cells contained 216 water molecules. After initial construction the systems were minimized and subjected to simulated annealing using 2000 steps of 1.0 fs each to approach 1000 K peak temperature before linearly cooling down to one of the seven target temperatures. Volume modification during simulated annealing was less than 1 % when compared to the box dimensions upon start-up. All calculations were performed with the TINKER package for molecular modeling version 4.2 [33].

2.2 MD/FEP Calculations

24 individual MD-trajectories per chosen target temperature (see section 2.1) were recorded. The TINKER package [33] was used for all computations. Polarizable AMOEBA force field parameters for water [21] were employed. AMOEBA works on the basis of self-consistent induced atomic dipoles. NpT ensembles were selected at 1.0 atm target pressure with the temperature/pressure coupling method due to Berendsen [34] which accounts for box-size changes when the volume of the repulsive cavity is introduced. Default coupling constants to the thermostat and barostat were used, that is 0.1 ps and 2.0 ps respectively. Other choices could have been made [35], especially with respect to the "Flying ice cube" phenomenon [36], but here we tried to follow closely the protocol used during AMOEBA development. Time steps of 1.0 fs were employed, no restraints/constraints were applied and Ewald summation was used. Two types of perturbation potentials were introduced,

$$V_{rep} = \lambda \left(\frac{B^*}{r} \right)^{12} \tag{1}$$

and

$$V_{rep}^{mod} = \frac{\lambda^{12}}{\left[0.3(1-\lambda)^2 + \left(\frac{r}{B^*=1.0} \right)^6 \right]^2} \tag{2}$$

to avoid discontinuities when the thermal radius of the repulsive cavity, B^*, approaches 0 Å [37, 38]. Parameter λ in equations (1) and (2) describes the degree of perturbation and assumes values from $\lambda = 0$ (unperturbed) to $\lambda = 1$ (fully perturbed). All technical details concerning the perturbation potential are given in [28]. Trajectories were recorded for 100 ps each and the perturbations shown in equations (1) and (2) were calculated and stored every time step. As reported previously, the $\lambda = 0.5$ simulation applying V_{rep}^{mod} of equation (2) is quasi-unperturbed and was used to monitor the time evolution of the macroscopic liquid water density. Data evaluation was started only after stable levels of the liquid water density had been reached (approximately after 40 to 50 ps, see Table 1). The $\lambda = 0.5$ simulation has also been analyzed with respect to maintainance and changes in the Hydrogen Bond network, as outlined in [41, 42] (see Supplementary Material).

2.3 Data Evaluation

For each of the 7 selected target temperatures (see section 2.1) the recorded 25 trajectories were used for application of Zwanzig's [10] formula

$$\Delta G(\lambda_i) = -k_B T \quad ln \left\langle e^{-\frac{1}{k_B T}[\mathcal{H}(\lambda_i+\delta\lambda)-\mathcal{H}(\lambda_i)]} \right\rangle_{\lambda_i} \tag{3}$$

with $< >$ depicting a thermodynamic average, k_B being the Boltzmann constant and $\mathcal{H}$ the total energy of the system. The average is formed at λ_i with small perturbations $\delta\lambda$ around λ_i. The OST is applied similarly to the description given in [28]. Care has been taken of using proper $k_B T$ factors for all the seven different temperatures mentioned above. This will effect equation (3) and the conversion from repulsive radii, B, to thermal radii, B^*, i.e. $B^* = B(1k_B T)^{-\frac{1}{12}}$. Perturbations exceeding energies of $2k_B T$ were not considered for total averages (FEP requirement). There are however always sufficiently enough alternative overlap combinations in all the simulations to smoothly connect two adjacent repulsive spheres and get statistical averages. Obtained raw data from the OST were fitted with polynomials of degree 2 and corresponding coefficients k_0, k_1 and k_2 are summarized in Table 1. Resulting cavitation free energies from the coefficients in Table 1 are expressed in units of kcal/mol (1 kcal = 4.184 kJ).

3 Results

3.1 AMOEBA based computer simulations of molecular liquid water confirm LCW ideas of the unit volume entropic change for solvating small-sized hydrophobic solutes

MD/FEP calculations based on the polarizable force field AMOEBA for the computation of cavitation free energies in liquid molecular water are carried out at seven different target tem-

peratures. The results are fitted similarly to previous calculations [28] and resulting coefficients k_0, k_1, k_2 are summarized in Table 1 (*revised Pierotti Approach*, rPA). The coefficients are used to calculate temperature trends for growing cavities of perfectly spherical shape. Figure 1 shows a comparison of these data in reduced energy units normalized to unit volumes. This type of reduced units allows one to immediately compare unit volumes of 1 cubic Å to each other. Unit volume cavitation free energies of small-sized cavities (squares and discs in Figure 1) clearly exhibit a positive slope for the tangent formed at room temperature data points. This indicates a drop in entropy for the process of hydrating a hydrophobic volume of 1 cubic Å. Similar constructions of tangents for larger-sized cavities (triangles and diamonds in Figure 1) show that the positive slopes become smaller as cavities grow. Thus high level force field based MD/FEP calculations verify the anticipated change in unit volume entropy following LCW theory for small-sized hydrophobic solutes (see for example Figure 2 in [29] for comparison to Figure 1 of the present work).

3.2 Cavitation entropies of small sized hydrophobic solutes decrease steadily with increasing cavity size

Equally interesting than unit volume entropies are the changes observed for full size cavitation, that is trends due to the creation of the entire cavity volume. Figure 2 shows the temperature trend of cavitation free energies of small sized hydrophobic solutes without scaling to the unit volume. Tangential lines formed at room temperature data points again exhibit positive slopes thus again indicating a drop in entropy. However, the magnitude of the slope becomes larger with increasing cavity size (e.g. compare slopes of tangential lines for small-sized cavities, squares and discs in Figure 2, to tangential slopes of larger-sized cavities, triangles and diamonds in Figure 2). Inversion in the sign of the slopes of tangential lines is seen close to the boiling point. Quantification of individual enthalpic and entropic contributions is given in Table 2. Small negatively signed values of ΔH are likely to result from numerical processing and should rather not taken to represent physical meaning. As may be seen from Table 2, the process is largely dominated from entropy and only to a minor extent enthalpic. Therefore we need to conclude that the change in entropy is steadily decreasing the larger the hydrophobic solute becomes.

3.3 Elevated temperature simulations of molecular liquid water largely resemble the experimentally observed temperature dependence of the liquid water density

In order to assure proper model description of intermolecular forces at temperatures other than room temperature, the macroscopic liquid water density is extracted from each simulation

performed at a certain target temperature. Figure 3 shows a comparison between simulation data (squares) and experimental measurements [30] (discs). Largest deviations occur at 300 K and 370 K with a maximum unsigned error of 0.01 $\frac{g}{cm^3}$ appearing at 300 K. The root mean square deviation amounts to 0.0056 $\frac{g}{cm^3}$. Given the rather close match at temperatures close to the boiling point, the overall rating of the simulations concerning intermolecular interactions at elevated temperatures must be considered very satisfactory. Consequently, taking the present data to form T-derivatives in order to determine entropic changes seems to be a valid approximation.

3.4 Rather close quantitative agreement between LCW predictions of the unit volume entropic change for the solvation of small-sized hydrophobic spheres and results derived from present computer simulations

Graphical extrapolation of unit volume ΔS values from the slopes of tangents formed at room temperature data points in temperature dependence plots of the unit volume ΔG^{cav} (Figure 1) yields the following values: $\Delta S_{B=2\mathring{A}} \approx$ -0.00027 $\frac{kcal/mol}{\mathring{A}^3 K}$, $\Delta S_{B=3\mathring{A}} \approx$ -0.00020 $\frac{kcal/mol}{\mathring{A}^3 K}$, $\Delta S_{B=4\mathring{A}} \approx$ -0.00015 $\frac{kcal/mol}{\mathring{A}^3 K}$ and $\Delta S_{B=5\mathring{A}} \approx$ -0.00012 $\frac{kcal/mol}{\mathring{A}^3 K}$. A similar evaluation of the data presented in [29] leads to comparable values, i.e. $\Delta S^{Huang,Chandler}_{B=3\mathring{A}} \approx$ -0.00007 $\frac{kcal/mol}{\mathring{A}^3 K}$. Thus present computer simulation data not only show qualitative agreement with LCW theory on the hydrophobic effect of small-sized solutes, but also lead to comparable results in absolute numbers of unit volume entropic changes.

3.5 Present computer simulations are limited to the small-size domain of hydrophobic hydration

rPA coefficients obtained from MD/FEP calculations in AMOEBA water are strictly valid only in the domain of existing FEP data. It is reasonable to extrapolate into the extended cavity size domain due to the smoothness of the data. However, after about B=5 Å (twice the radius of the largest accumulated perturbation) any further usage is certainly speculative. Therefore it was surprising to see indications of general applicability even in largely extended cavity domains [14]. In order to probe the quality of large scale extrapolation the temperature trend of the surface tension, σ, is shown in Figure 4 and compared to experimental data [31]. Approximation of σ from the present rPA data is critical (see Discussion). It involves limit value consideration of $\lim_{B\to\infty} \Delta G^{cav}/(4\pi B^2)$ [14] and the presented data is due to setting B=100 Å, hence clearly an extrapolation to large scale. Figure 4 shows that the calculated surface tensions are close to

the experimental values but do not reproduce the correct trend with increasing temperature, demonstrating the anticipated uncertainty with large-size approximations.

3.6 Analysis of the hydrogen bond network as determined by the ensemble of snapshot structures obtained from AMOEBA based MD simulations goes hand in hand with recently reported findings of experimental as well as theoretical studies

MD/FEP runs carried out at $\lambda = 0.5$ (quasi-unperturbed) are examined with respect to structural relationships maintained between individual water molecules. Corresponding sets of saved snapshot structures of individual water boxes at T=300 K and T=370 K are analyzed. The three basic *Radial Distribution Functions* (RDF) that characterize the "fine structure" of bulk water are derived and corresponding trends shown in the Supplementary Material, Figures A-C (300 K) and Figures D-F (370 K). RDFs from the present data reproduce those reported in the original AMOEBA paper (see [21] Figures 5 – 7) very well. The RDF of the oxygen-oxygen distance, $g_{OO}(r)$, shows the characteristic immediate neighborhood peak at 2.9 Å and a second very diffuse peak around 4.6 Å which is hardly distinguishable from the baseline. The second peak in the $g_{OH}(r)$ — due to pairs of water molecules directly associated via hydrogen bonds (HBs) — appears at 1.9 Å in the present data. The $g_{HH}(r)$ exhibits a characteristic second peak at 2.5 Å. Following the procedure devised in [42] for geometrical constraints defining a particular HB we determine an average number of established HBs of 1.6 per water molecule in the 300 K simulation data. The frequency of tetrahedral coordination mediated by HBs is only on the order of 2 % at this simulation temperature. This seems to be consistent with the experimental study of Wernet et al [41] where the conclusion was drawn that bulk water predominantly exists in a state with 2 HBs established per water molecule. The present data is also in close agreement with the MP2 results of the QM/MM study by Xenides et al [42]. Significant changes observed at the high temperature simulation of T=370 K include the entire loss of the second broad shoulder around 4.6 Å in the $g_{OO}(r)$, the decrease of the average number of HBs to 1.4 per water molecule and the general loss of tetrahedral coordinations mediated by HBs.

4 Discussion

The present study has employed the high level polarizable AMOEBA force field for computer simulation of liquid water [21] at several temperatures and normal pressure. We are interested in the free energy cost of creation of small-sized cavities, which are model constructs for hydrophobic molecules. A first requirement was to show that intermolecular relationships are still maintained at reasonable physical conditions upon temperature increase [15]. A rather direct

evidence in this regard is the relatively close match between simulated and experimental data of the liquid water density shown in Figure 3. Next the temperature profile of ΔG was used to get estimates for the unit volume ΔS (Figure 1) as well as for the full size ΔS of cavitation (Figure 2). Computer simulation values for ΔS can be derived from the negative slope of the tangents constructed at a certain temperature. In so doing the ΔS for room temperature hydrophobic hydration of small-sized molecules was shown to exhibit a negative sign, which was predicted previously from LCW-theory [4]. The absolute value of the change in cavitation entropy, ΔS, becomes larger with increasing size of the hydrophobic molecule (see Figure 2 and Table 2). Tendency inversion is observed only at elevated temperatures close to the boiling point.

In general, the LCW picture of the unit volume hydrophobic effect of small-sized solutes is very well reproduced (see for example Figure 2 in [29]). Small differences include, the exact position of the maximum, which occurs closer to the boiling point in the present data, the quantification of the unit volume ΔS, which leads to higher values in the present study and the continuity of the onset of the curves at temperatures close to the freezing point, which is steady here, but shows some inversion at B=4 Å solutes in LCW-theory. Extrapolation of the present data to very large solute sizes is impossible as seen from the wrong prediction of the temperature profile of the surface tension (Figure 4). The present approach has made use of a very expensive computational technique (Ewald sum MD/FEP within the OST) and could only be carried out under massive employment of grid computing [27]. All final rPA coefficients corresponding to all the considered temperatures are summarized in Table 1. It is interesting to note, that all present k_0, k_1, k_2 coefficients derived for 300 K lead to only minor alterations in the data presented recently in [14] that were based on non-Ewald simulations, but application of plain periodic boundary conditions instead [23].

An interesting observation made in the present work is the fact that the overall entropy of hydrophobic hydration is steadily decreasing with growing solute size (see Figure 2 and Table 2). This is somewhat contradictory with the LCW-picture of the anticipated change in the sign of ΔS when the solutes are thought to cross over from small length scales (volume dependence) to large length scales (surface area dependence). The critical crossover dimension was approximated to be on the order of 10 Å of radial extension of the hydrophobic solute [4]. On the other hand, strictly speaking, the crossover region is beyond the reach of the current data set and firm statements can only be made upon extension of the present approach into the critical domain of crossover length scales. This would however involve an even bigger initiative of supercomputing with unforeseeable complexity. It is still interesting to note that an extension of the rPA approach into medium length scales was recently shown to be not entirely unreasonable when operating with the solvent excluded volume [14].

Predicting the temperature dependence of the surface tension (see Figure 4) from present rPA data failed. First of all it should be noted, that surface tension per se is appropriate for the description of water embedded macroscopic bubbles. These bubbles are fundamentally different to cavities of comparable size, because the latter are strictly empty. Therefore, all what makes a

bubble stabilize, i.e. the vapour-like molecules in the interior bouncing back and fourth against the bubble walls, will be completely missing in a cavity, because the cavity interior is void. Nevertheless, the equivalence in units of surface-normalized cavitation free energies on the one side and surface tensions on the other side, makes it attractive to try the prediction of the latter via $\lim_{B\to\infty} \Delta\ G^{cav}/(4\pi\ B^2)$. However, the energy in the context of surface tension implies an energy required to maintain the liquid-vapour coexistence of a bubble, while it expresses an amount of clearance work to create the empty space in a cavity. These two different types of energies should not be confused with each other and in principle, need not even be correlated. Thus the rather successful match of $\lim_{B\to\infty} \Delta\ G^{cav}/(4\pi\ B^2)$ with the experimental surface tension of water reported in [14] could also be purely fortuitous. On the other hand it could also explain why surface tension based solvation models [32] and LCW-theory have become so successful. LCW theory — like the earlier concepts introduced by Kauzmann [39] and Tanford [40] — build upon oil/water surface tension and explain the switch in sign of ΔS for the hydration of hydrophobic solutes of increasing size by the experimental temperature dependence of surface tensions. LCW in particular has proclaimed that such a switch in sign would occur at spherical volumes of radial dimension on the order of 10 Å. Taking up this idea, ΔS values in the vicinity of the 10 Å domain should smoothly become smaller and smaller before they reach zero and then start to assume negative values. A plot of ΔS in this critical region should therefore certainly not exhibit characteristics of a monotonic growth, otherwise the transition would have to occur discontinuously. In the present study, although still operating far away from the critical domain of 10 Å, we do however observe signatures of a monotonic growth (see Table 2). This will be of particular interest to examine in closer detail from extended studies of the type presented here.

5 Conclusion

In summary, evidence has been presented that the hydrophobic effect of small-sized solutes is due to the drop in entropy. The insight gained here is also an encouraging sign that high level force fields are approaching now standards that allow one to study effects beyond the reach of experimental methods.

Acknowledgements The authors are grateful for having been granted all necessary computer time by the Austrian Grid [27]. This work was supported in part by the National Institutes of Health Grant GM62838. The authors thank Petra Bareis and Roland Felnhofer from the Novartis Institutes for BioMedical Research, Vienna, for their collaborative spirit.

References

[1] D. Chandler, *Nature*, 2005, **437**, 640.

[2] P. Liu, X. Huang, R. Zhou, B. J. Berne, *Nature*, 2005, **437**, 159.

[3] F. Despa, A. Fernández, R. S. Berry, *Phys. Rev. Lett.*, 2004, **93**, 228104.

[4] K. Lum, D. Chandler, J. D. Weeks, *J. Phys. Chem. B*, 1999, **103**, 4570.

[5] L. R. Pratt, A. Pohorille, *Proc. Natl. Acad. Sci.* USA, 1992, **89**, 2995.

[6] G. Hummer, S. Garde, A. E. Garcia, A. Pohorille, L. R. Pratt, *Proc. Natl. Acad. Sci.* USA, 1996, **93**, 8951.

[7] F. M. Floris, M. Selmi, A. Tani, J. Tomasi, *J. Chem. Phys.*, 1997, **107**, 6353.

[8] N. Choudhury, B. M. Pettitt, *J. Am. Chem. Soc.*, 2005, **127**, 3556.

[9] H. S. Ashbaugh, M. E. Paulaitis, *J. Am. Chem. Soc.*, 2001, **123**, 10721.

[10] R. W. Zwanzig, *J. Chem. Phys.*, 1954, **22**, 1420.

[11] P. M. Postma, H. J. C. Berendsen, J. R. Haak, *Farad. Symp. Chem. Soc.*, 1982, **17**, 55.

[12] T. Simonson, G. Archontis, M. Karplus, *Acc. Chem. Res.*, 2002, **35**, 430.

[13] J. Tomasi, B. Mennucci, R. Cammi, *Chem. Rev.*, 2005, **105**, 2999.

[14] S. Höfinger, F. Zerbetto, *Chem. Soc. Rev.*, 2005, **34**, 1012.

[15] D. Paschek, *J. Chem. Phys.*, 2004, **120**, 6674.

[16] P. E. Krouskop, J. D. Madura, D. Paschek, A. Krukau, *J. Chem. Phys.*, 2006, **124**, 016102-[1,2].

[17] R. Zhou, X. Huang, C. J. Margulis, B. J. Berne, *Science*, 2004, **305**, 1605.

[18] M. R. Shirts, V. S. Pande, *J. Chem. Phys.*, 2005, **122**, 134508.

[19] W. L. Jorgensen, J. Chandrasekhar, J. D. Madura, R. W. Impey, M. L. Klein, *J. Chem. Phys.*, 1983, **79**, 926.

[20] H. J. C. Berendsen, J. P. M. Postma, W. F. van Gunsteren, J. Hermans, *Intermolecular Forces;* Reidel Publishing Company: Dordrecht, the Netherlands, 1981.

[21] P. Ren, J. W. Ponder, *J. Phys. Chem. B*, 2003, **107**, 5933.

[22] P. Ren, J. W. Ponder, *J. Phys. Chem. B*, 2004, **108**, 13427.

[23] S. Höfinger, F. Zerbetto, *Chem. Eur. J.*, 2003, **9**, 566.

[24] T. Ghosh, A. E. Garcia, S. Garde, *J. Chem. Phys.*, 2002, **116**, 2480.

[25] S. Rajamani, T. M. Truskett, S. Garde, *Proc. Natl. Acad. Sci.* USA, 2005, **102**, 9475.

[26] B. Almeida, R. Mahajan, D. Kranzlmüller, J. Volkert, S. Höfinger, *Lect. Notes. Comp. Sci.* 2005, **3666**, 433.

[27] J. Volkert, D. Kranzlmüller, *OCG Journal*, 2005, **1**, 4.

[28] S. Höfinger, F. Zerbetto, *Theor. Chem. Acc.*, 2004, **112**, 240.

[29] D. M. Huang, D. Chandler, *Proc. Natl. Acad. Sci.* USA, 2000, **97**, 8324.

[30] http://www.thermexcel.com ThermExcel Copyright © 2003-2004 by ThermExcel

[31] http://www.iapws.org/relguide/surf.pdf *IAPWS, International Association for the Properties of Water and Steam.* 1994

[32] C. J. Cramer, D. G. Truhlar, *Chem. Rev.*, 1999, **99**, 2161.

[33] J. W. Ponder, TINKER Copyright © 1990-2004 by Jay William Ponder

[34] H. J. C. Berendsen, J. P. M. Postma, W. F. van Gunsteren, A. DiNola, J. R. Haak, *J. Chem. Phys.*, 1984, **81**, 3684.

[35] H. C. Andersen, *J. Chem. Phys.*, 1980, **72**, 2384.

[36] S. C. Harvey, R. K. Z. Tan, T. E. Cheatham III, *J. Comp. Chem.*, 1998, **19**, 726.

[37] T. C. Beutler, A. E. Mark, R. C. van Schaik, P. R. Gerber, W. F. van Gunsteren, *Chem. Phys. Lett.*, 1994, **222**, 529.

[38] T. Simonson, *Mol. Phys.*, 1993, **80**, 441.

[39] W. Kauzmann, *Adv. Protein Chem.*, 1959, **14**, 1.

[40] C. Tanford, *The hydrophobic effect — formation of micelles and biological membranes;* Wiley: New York, 1973.

[41] Ph. Wernet, D. Nordlund, U. Bergmann, M. Cavalleri, M. Odelius, H. Ogasawara, L.Å. Näslund, T.K. Hirsch, L. Ojamäe, P. Glatzel, L.G.M. Pettersson, A. Nilsson, *Science*, 2004, **304**, 995.

[42] D. Xenides, B.R. Randolf, B.M. Rode, *J. Chem. Phys.*, 2005, **122**, 174506.

Table 1: Summary of the data resulting from free energy perturbation calculations of repulsive spheres in water at various simulation temperatures. Equilibration values of liquid water densities (second column) are derived from $\lambda = 0.5$ runs (quasi-unperturbed) after neglecting an initial fraction of the data set (fourth column). The data are fitted with polynomials of 2^{nd} degree [28] and resulting rPA-coefficients k_0, k_1 and k_2 are included in columns 5-7.

T	ρ_{sim}	ρ_{exp}	Initial Discard	rPA-Coefficients [14]		
				k_0	k_1	k_2
[K]	$[\frac{\text{g}}{\text{cm}^3}]$	$[\frac{\text{g}}{\text{cm}^3}]$	[ps]	[kcal/mol]	$[\frac{\text{kcal/mol}}{\text{Å}}]$	$[\frac{\text{kcal/mol}}{\text{Å}^2}]$
277	0.995	1.000	40	0.456 ± 0.015	-1.602 ± 0.062	1.116 ± 0.082
300	1.006	0.996	40	0.427 ± 0.012	-1.594 ± 0.044	1.183 ± 0.046
315	0.997	0.992	40	0.418 ± 0.041	-1.613 ± 0.060	1.220 ± 0.022
330	0.988	0.985	40	0.398 ± 0.008	-1.607 ± 0.045	1.236 ± 0.052
345	0.980	0.977	40	0.405 ± 0.011	-1.607 ± 0.045	1.251 ± 0.045
365	0.963	0.964	40	0.383 ± 0.015	-1.580 ± 0.026	1.262 ± 0.038
370	0.953	0.960	50	0.411 ± 0.009	-1.611 ± 0.037	1.236 ± 0.029

Table 2: Decomposition of cavitation free energies ΔG^{cav} (column to the right) of small-sized spherical volumes of radius B (leftmost column) into entropic (third column) and enthalpic (second column) fractions. The defragmentation is based on initial finite difference determination of ΔS from the temperature trend of ΔG^{cav} (see Figure 2) with subsequent trivial derivation of ΔH. The analysis is made for room temperature behaviour (T=300 K).

B [Å]	ΔH [kcal/mol]	$-T\Delta S$ [kcal/mol]	ΔG^{cav} [kcal/mol]
2	-0.728	2.699	1.972
3	-0.335	6.628	6.293
4	0.798	12.183	12.981
5	2.672	19.364	22.036

List of Figures

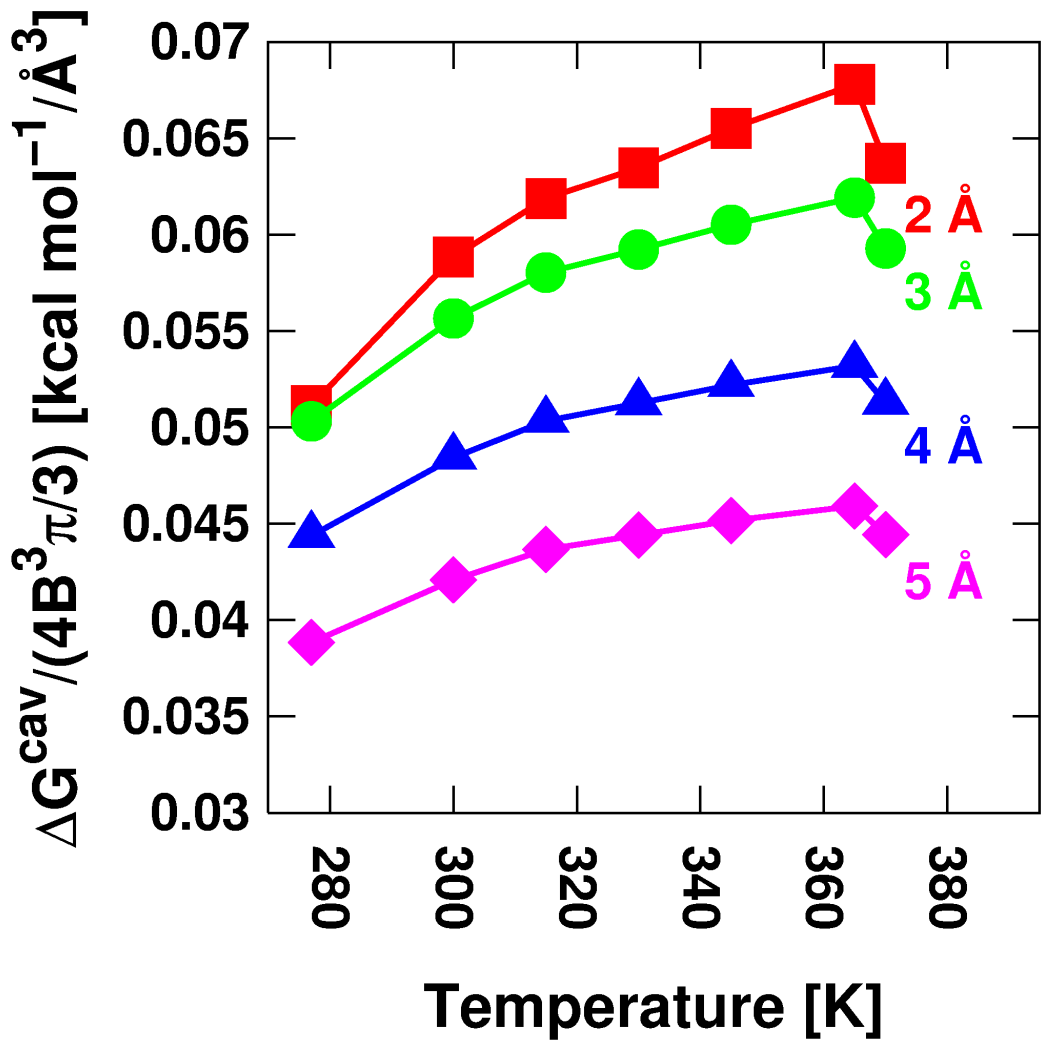

Figure 1: Temperature dependence of the unit volume free energy of cavitation for small repulsive spheres of growing size. Small-sized cavities of radii B = 2 Å (squares) and B = 3 Å (discs) exhibit room temperature tangents with positive slope that correspond to a unit volume ΔS of negative sign. Similar analysis of tangential slopes for larger volumes, i.e. B = 4 Å (triangles) and B = 5 Å (diamonds) demonstrates that the magnitude of the slopes decreases at 300 K when the size of the solute becomes bigger.

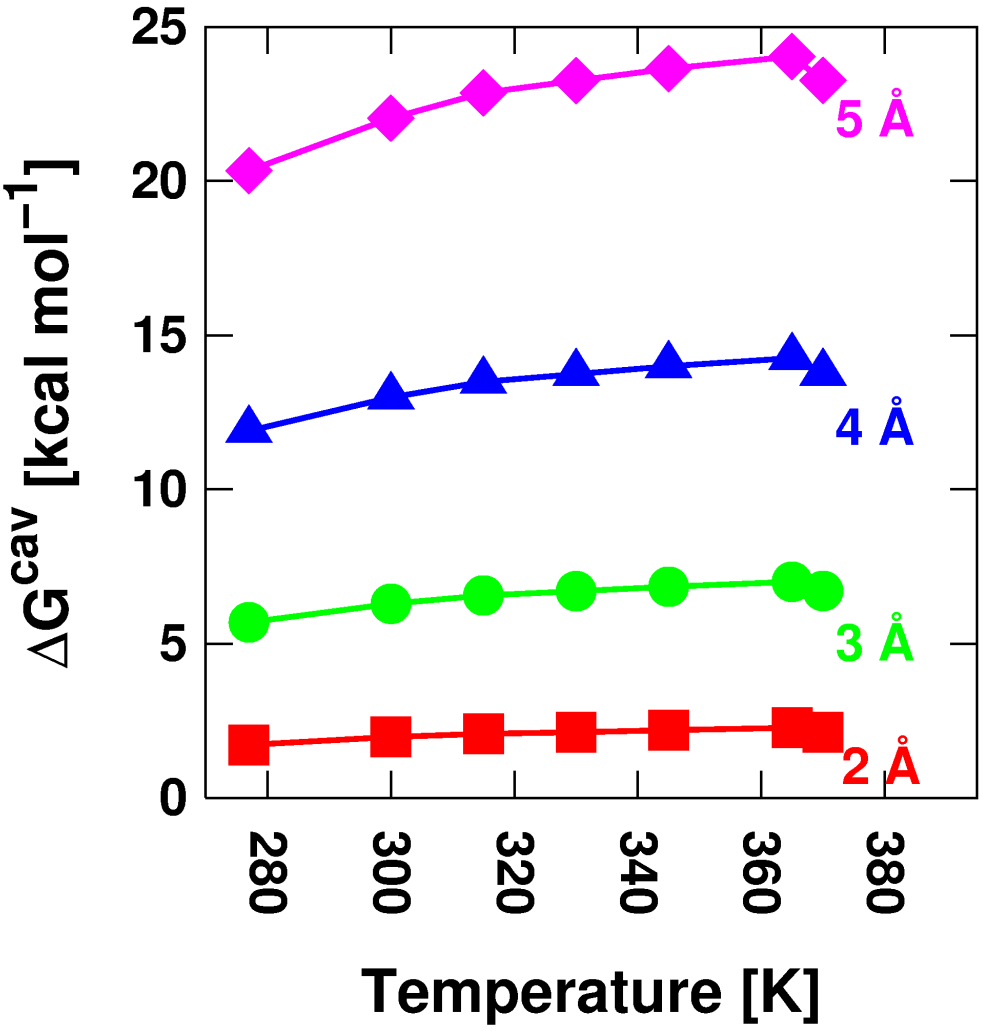

Figure 2: Temperature dependence of the full size free energy of cavitation for small repulsive spheres of growing size. Room temperature tangents exhibit positive slopes that correspond to a ΔS of cavitation of the entire cavity volume with negative sign. The magnitude of the slope of tangential lines increases with growing cavity size, i.e. when following cavities of radii B = 2 Å (squares), B = 3 Å (discs), B = 4 Å (triangles) and B = 5 Å (diamonds). Inversion in the sign of the slopes of tangential lines is seen close to the boiling point.

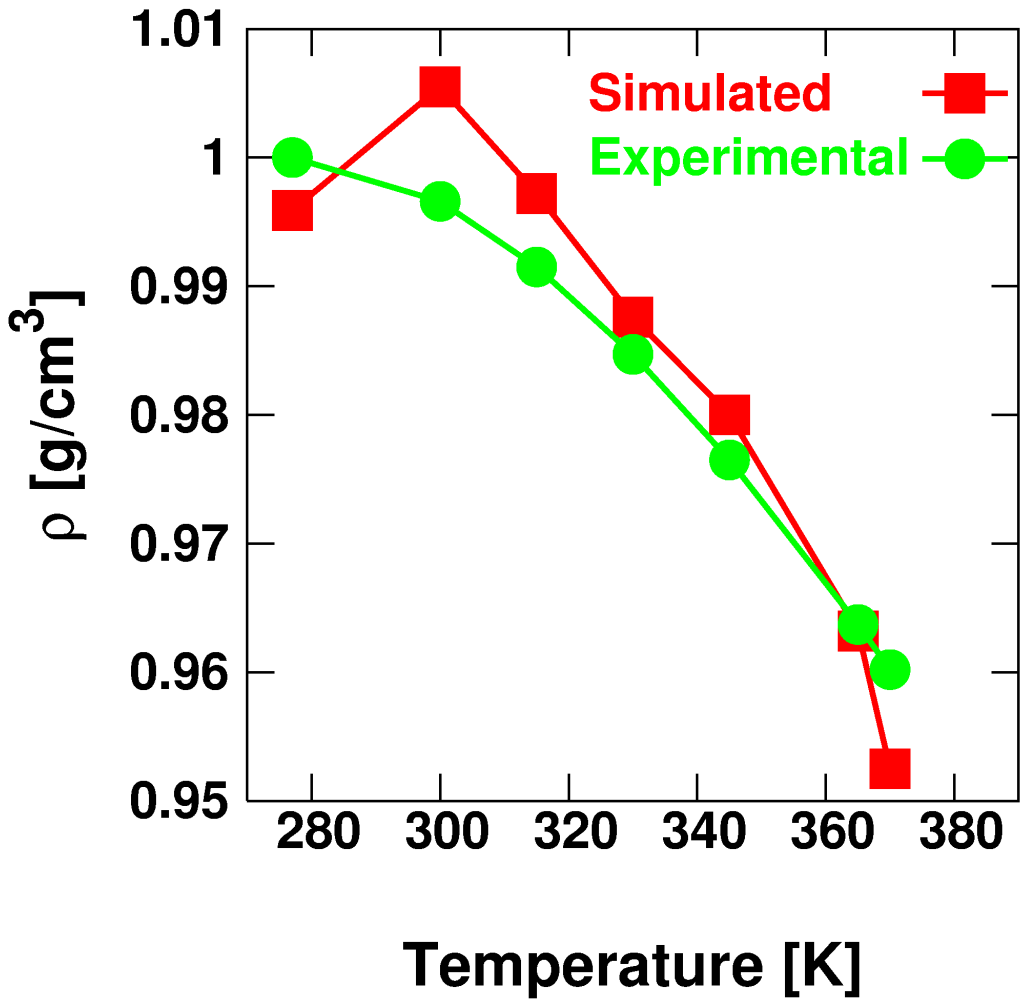

Figure 3: Comparison of simulated and measured macroscopic density, ρ, of liquid water at various temperatures. The simulated water densities (squares) are derived from λ=0.5 MD/FEP calculations that take place quasi-unperturbed [23]. The experimental densities (discs) are obtained from standard tabulations [30]. Greatest deviations from experimental values occur at 300 K and 370 K. The root mean square deviation is 0.0056 g cm^{-3}.

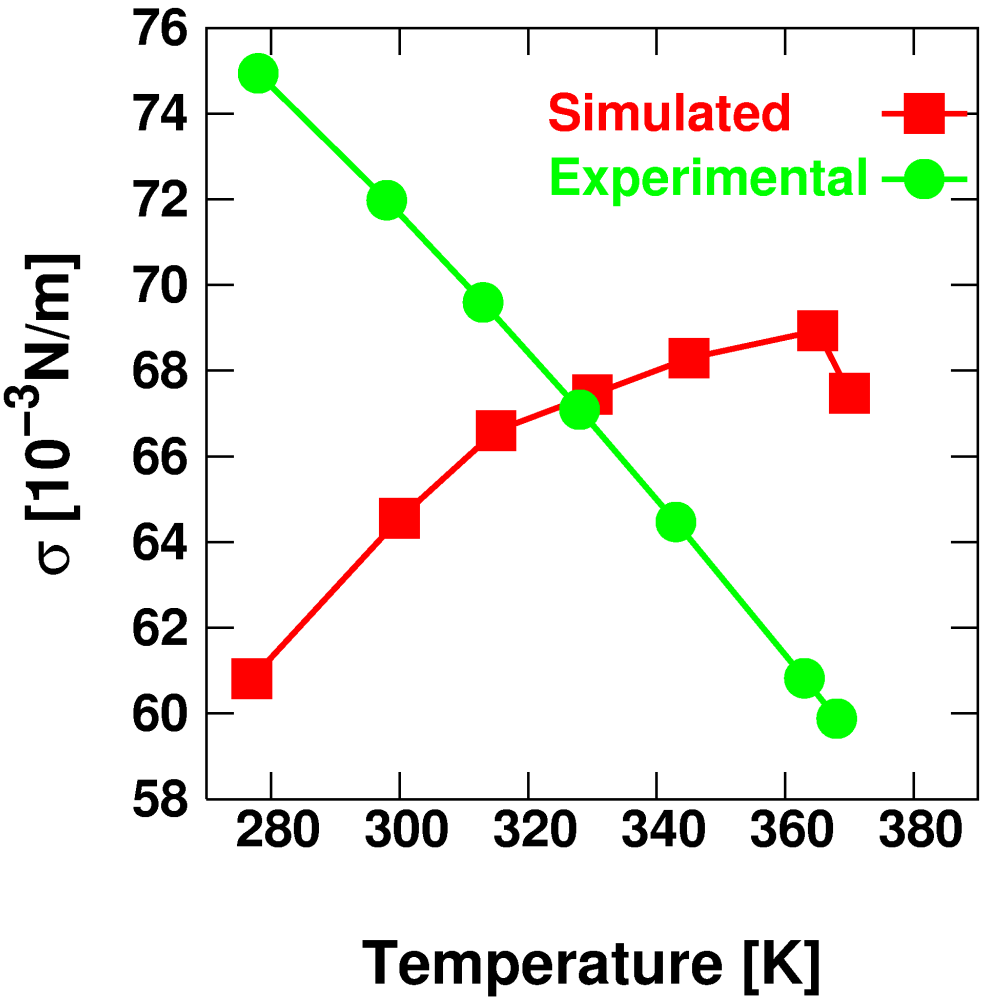

Figure 4: Comparison of simulated and measured surface tension, σ, of liquid water at various temperatures. The calculated values of σ (squares) are due to $\lim_{B\to\infty} \Delta\ G^{cav}/(4\pi\ B^2)$ with B=100 Å. Experimental reference data (discs) have been obtained from standard tabulations [31]. Although qualitatively comparable, the calculated values of σ exhibit inverse temperature profiles, which might be an artefact stemming from large-scale extrapolation.